

ASCENT OF A TURBULENT AXISYMMETRIC THERMAL  
IN A NONUNIFORM COMPRESSIBLE ATMOSPHERE

G. M. Makhviladze, O. I. Melikhov,  
and S. E. Yakush

UDC 551.511+551.558.1+536.253

An entire range of physical and mechanical effects accompanies the evolution of clouds of light or heavy gas formed in the atmosphere in a gravitational field. Examples of such clouds are those formed by volcanic eruptions, surface and air explosions, and sudden releases of gases in industrial operations. The study of these effects is important for the solution of important problems in ecology, atmospheric physics, vulcanology, the theory of combustion and explosion, and explosion and fire safety.

The motion of a cloud of hot gas (a thermal) in a stably stratified atmosphere has been studied by many investigators both experimentally and theoretically. Three main stages of ascent of the thermal are usually distinguished. In the initial stage, a toroidal vortical flow is formed. Heated gas rising due to buoyancy induces motion in the surrounding medium. Here, the cloud acquires its characteristic mushroom shape, with a sharp leading temperature edge. In the next stage of ascent, the shape of the cloud remains roughly the same, while the coordinate of its upper edge increases over time in accordance with the law  $z_e \sim t^{1/2}$ . This stage has been termed the similarity stage, although a similarity solution leading to a fundamental law of ascent has been constructed only in a Boussinesq approximation for the case of uniform atmospheric stratification. Finally, at the concluding stage of motion of the thermal, the presence of stable atmospheric stratification leads to slowing of the ascent and suspension of the gas. Here, the thermal undergoes decaying oscillations about the point of suspension.

The dynamics of the ascent of thermals was first studied with the use of unidimensional models which employed characteristics of the cloud averaged over its volume and entailed additional hypotheses on the character of entrainment of the environment into the body of the thermal [1-3]. More complete multidimensional models were studied by asymptotic and approximate methods. With the development of computer technology, it became possible to perform detailed numerical calculations of the evolution of thermals. Meanwhile, most investigations used the system of equations of an incompressible fluid in the Boussinesq approximation. The most complete analytic and numerical study of an axisymmetric turbulent thermal on the basis of this model was completed in [4]. Each stage was examined separately, and the different solutions were joined together.

Calculations based on the Navier—Stokes system of equations for a compressible gas have been used to study the beginning of motion — the formation of a vortex ring [5, 6] — as well as the ascent and interaction of a pair of thermals [7], physicochemical processes in thermals due to the presence of a chemically active or inert disperse impurity in the cloud [8, 9], the thermal-type flow which develops in the combustion of a horizontal layer of fuel [10], and the removal of aerosol particles into the stratosphere by a hot thermal [11]. A more detailed review and bibliography are given in [4, 12].

It should be noted that despite the substantial number of studies devoted to the numerical modeling of the evolution of thermals, it is of great interest to study more complete and more complex models which consider both thermal and gravimetric compressibility, the presence of an underlying surface and wind, and the effect of different degrees of temperature stratification of the atmosphere. The choice of the effective transport coefficients, accounting for the turbulent character of the flow, must be substantiated. It is also necessary to develop numerical methods that will make it possible to completely calculate convective flows in the atmosphere with a large vertical scale.

Here, we use the Navier—Stokes equations for a viscous and compressible thermally conducting gas to numerically study the ascent of an axisymmetric turbulent thermal in a stratified atmosphere. The values of the turbulent transport coefficients are chosen from the

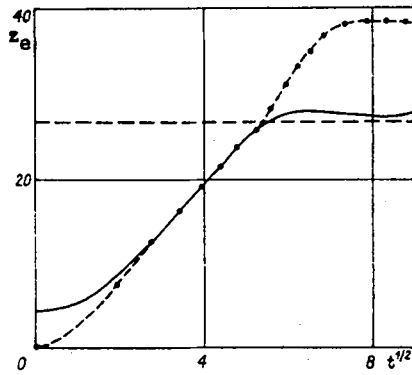


Fig. 1

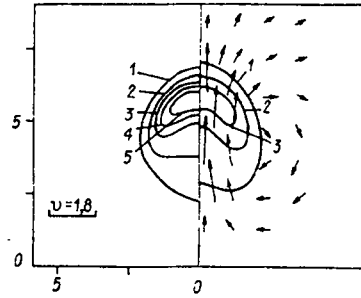


Fig. 2

condition of agreement between experimental relations and a theoretical law describing the ascent of the upper edge of a thermal at the similarity stage of motion.

1. Let a stationary spherical cloud of heated gas (thermal) form at the initial moment above a plane horizontal surface. Under the influence of buoyancy, the cloud begins to rise. The problem consists of calculating all stages of evolution of the thermal up to the point of temperature equalization.

We introduce a cylindrical coordinate system  $(r, z)$  whose origin lies on the underlying surface under the center of the thermal. We also introduce dimensionless variables, having chosen as scales the initial radius of the cloud  $R$  and the velocity  $\sqrt{Rg}$ , time  $\sqrt{R/g}$ , density, temperature, and pressure of the undisturbed atmosphere at the surface  $\rho_0, T_0, p_0 = \rho_0 R_0 T_0$  (the gas is assumed to be ideal;  $g$  is acceleration due to gravity;  $R_0$  is the gas constant).

The nonsteady axisymmetric motion of a viscous, compressible, thermally-conducting gas in dimensionless variables is described by the following system of equations:

$$\frac{d\rho}{dt} + \rho \operatorname{div} \mathbf{U} = 0 \quad \left( \frac{d}{dt} = \frac{\partial}{\partial t} + (\mathbf{U} \cdot \nabla) \right); \quad (1.1)$$

$$\rho \frac{d\mathbf{U}}{dt} = -\frac{1}{\gamma M^2} \nabla p + \rho \mathbf{f} + \frac{1}{\operatorname{Re}} \left[ \Delta \mathbf{U} + \frac{1}{3} \nabla (\operatorname{div} \mathbf{U}) \right]; \quad (1.2)$$

$$\rho \frac{dT}{dt} = -(\gamma - 1) p \operatorname{div} \mathbf{U} + \frac{\gamma}{\operatorname{Re} \operatorname{Pr}} \Delta T, \quad p = \rho T; \quad (1.3)$$

$$M^2 = Rg/\gamma R_0 T_0, \quad \operatorname{Re} = R \sqrt{Rg} \rho_0/\eta, \quad \gamma = c_p/c_v, \quad (1.4)$$

$$\operatorname{Pr} = c_p \eta/\lambda, \quad \mathbf{f} = (0, -1), \quad \mathbf{U} = (u, v), \quad \Delta = \frac{1}{r} \frac{\partial}{\partial r} r \frac{\partial}{\partial r} + \frac{\partial^2}{\partial z^2},$$

where  $t$  is time;  $\rho, \mathbf{U}, p$ , and  $T$  are the density, velocity, pressure, and temperature of the gas;  $M, \operatorname{Re}$ , and  $\operatorname{Pr}$  are the Mach, Reynolds, and Prandtl numbers;  $\eta$  and  $\lambda$  are absolute viscosity and thermal conductivity;  $c_p$  and  $c_v$  are the heat capacities of the gas at constant pressure and constant volume.

For the clouds being examined, having the radius  $R \sim 10^2 - 10^3$  m and an initial temperature  $T_c \sim (10-20)T_0$  at their center, the Reynolds number obtained from the molecular viscosity of air  $\operatorname{Re} \sim 10^8 - 10^{10}$  ( $\eta/\rho_0 \sim 10^{-1}$  cm<sup>2</sup>/sec). The Rayleigh number, characterizing the rate of convection, is  $\operatorname{Ra} = \operatorname{Re}^2 \operatorname{Pr} (T_c - T_0)/T_0 \sim 10^{17} - 10^{21}$ . As experiments have shown [4], motion is of a developed turbulent character at such values of  $\operatorname{Ra}$ . This is taken into account by introducing effective ("turbulent") constant values in place of the laminar transport coefficients. Thus, the values of  $\operatorname{Re}$  and  $\operatorname{Pr}$  in (1.2), (1.3) represent turbulence analogs of the corresponding laminar criteria.

The evolution of the cloud is conveniently followed by introducing a passive (not having a reciprocal effect on the motion of the gas) impurity whose concentration  $c = \rho_2/\rho$  ( $\rho_2$  is the density of the impurity) satisfies the equation of convective turbulent diffusion

$$\frac{\partial \rho c}{\partial t} + \operatorname{div} (\rho c \mathbf{U}) = \frac{1}{\operatorname{Re} \operatorname{Sc}} \Delta c. \quad (1.5)$$

In (1.5), it was assumed that the diffusion coefficient  $D \sim 1/\rho$ , while  $\operatorname{Sc} = \eta/\rho D$  is the turbulence analog of the Schmidt number. In the calculations, we took  $\operatorname{Sc} = \operatorname{Pr}$ .

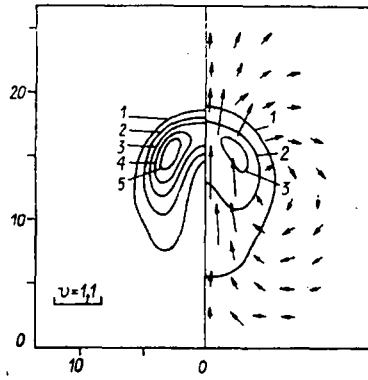


Fig. 3

The initial conditions have the form

$$\begin{aligned} t = 0, T(r, z) &= T_a(z) + \Theta_0 \exp[-(r^2 + (z - H)^2)], \\ p(r, z) &= p_a(z), \rho_2(r, z) = \exp[-(r^2 + (z - H)^2)], \\ U = 0, \rho(r, z) &= p(r, z)/T(r, z), \end{aligned} \quad (1.6)$$

which corresponds to a stationary spherical cloud of heated gas located at the altitude  $H$ . The spatial distribution of the excess temperature is Gaussian, the characteristic radius of this distribution having been chosen as the length scale. In (1.6),  $T_a$  and  $p_a$  are the height-wise distributions of the temperature and pressure of the undisturbed atmosphere;  $\Theta_0$  is the initial excess temperature at the center of the thermal.

The boundary conditions account for the symmetry on the axis and adhesion of the gas to the underlying surface, which is adiabatic and impermeable for the passive impurity. The boundary conditions also include the absence of perturbations at infinity. The conditions are written in the form

$$\begin{aligned} r = 0, u = 0, \partial\varphi/\partial r &= 0 \quad (\varphi = \{\rho, v, p, T, c\}), \\ z = 0, U = 0, \partial T/\partial z &= 0, \partial c/\partial z = 0, r^2 + z^2 \rightarrow \infty, U = 0, \\ p &= p_a, T = T_a, \rho = \rho_a, c = 0. \end{aligned} \quad (1.7)$$

The temperature stratification of the atmosphere was assigned in accordance with the model of the international standard atmosphere [4]. In dimensional variables

$$\frac{g}{T_a} \left( \frac{dT_a}{dz} + \frac{g}{c_p} \right) = N^2 \quad (1.8)$$

(the parameter  $N^2$  determines the stratification of the medium). Up to the tropopause (its altitude  $H_t = 10$ – $16$  km, depending on the latitude and time of year),  $N^2 = N_1^2 = \text{const} = 1.2 \cdot 10^{-4} \text{sec}^{-2}$ . Above the tropopause,  $N^2 = N_2^2 = \text{const} = 4.4 \cdot 10^{-4} \text{sec}^{-2}$ . In dimensionless variables, Eq. (1.8) takes the form

$$\frac{1}{T_a} \left( \frac{dT_a}{dz} + (\gamma - 1) M^2 \right) = k, \quad k = N^2 R/g.$$

The pressure distribution  $p_a(z)$  was found from the known temperature field  $T_a(z)$  by integration of the equation of hydrostatic equilibrium  $dp_a/dz = -\gamma M^2 \rho_a = -\gamma M^2 p_a/T_a$  ( $\rho_a$  is the density distribution of the undisturbed atmosphere).

It should be noted that the compressible-medium model being considered makes it possible to correctly describe the initial section of the ascent of a thermal when there is a large difference between the densities of the thermal and the surrounding atmosphere (the Boussinesq approximation being invalid). The model also allows description of the evolution of large thermals rising to great altitudes, when a large role begins to be played by static (gravimetric) compressibility — the change in the density of the atmosphere with altitude.

2. In selecting the values of  $Re$  and  $Pr$ , we used an approach similar to that developed in [4]. As experiments have shown, the following relation is valid on the similarity section of the ascent

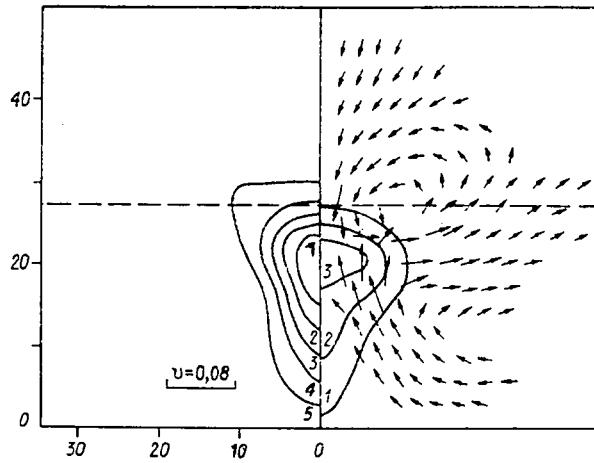


Fig. 4

$$z_e - z_0 \approx 4.35 \Pi_0^{1/4} t^{1/2}, \quad (2.1)$$

where  $z_e$  is the coordinate of the upper edge;  $z_0$  is the position of the virtual source;  $\Pi_0$  is the initial reserve buoyancy of the cloud [4, 13]. Thus, the theoretical turbulent transport coefficients can be chosen by comparing the similarity coordinate of the upper edge  $\zeta_e = (dz_e/dt^{1/2}) \Pi_0^{-1/4}$  with the experimental value  $\zeta_e \approx 4.35$ .

The value of  $\Pi_0$ , calculated in terms of the heat of formation of the thermal  $Q_0$  from the formula  $\Pi_0 = g\beta Q_0 / (2\pi\rho_a c_p)$  ( $\beta = 1/T_a$ ), in an analysis of empirical data in [4, 13], occurs naturally in the use of the Boussinesq approximation: in this case, buoyancy is the motion integral for the initial and similarity stages together with  $Q_0$ . It was shown in

[12] that, for a compressible gas, only the thermal energy  $Q_0 = 2\pi \int_0^\infty \int_0^\infty \rho c_p (T - T_a) r dr dz$  is con-

served at these stages. With the intention of comparing the results of calculations of the motion of a thermal in a compressible medium with empirical relation (2.1), we transform the latter so as to include the energy  $Q_0$  conserved during the process. Then  $z_e - z_0 \approx 4.35 \times \left( \frac{g\beta}{2\pi\rho_a c_p} Q_0 \right)^{1/4} t^{1/2}$  or, in the dimensionless variables introduced in Part 1,

$$z_e - z_0 \approx 4.35 I_0^{1/4} t^{1/2}, \quad I_0 = \int_0^\infty \int_0^\infty \rho (T - T_a) r dr dz, \quad (2.2)$$

Here,  $\zeta_e = (dz_e/dt^{1/2}) I_0^{-1/4}$ . Empirical relation (2.2) was used to select theoretical values of Re and Pr by comparison with a sufficiently general criterional relation calculated in [12] and having the form  $\zeta_e = f(\text{Gr}, H)$ ,  $\text{Gr} = \text{Ra}/\text{Pr}$ . This relation is valid with a broad range of initial conditions. The question of the determination of turbulent transport coefficients that will ensure agreement of the law of ascent of the upper edge of the cloud with experimental findings was examined in detail in [4, 12] for compressible and incompressible media, respectively.

Problem (1.4)-(1.7) was solved numerically by a finite-difference method using an implicit three-level branching scheme [14] which was modified in [12] to improve the conservative properties. The calculations were performed on moving nonuniform  $40 \times 50$  grids with the use of a variable time step. Calculation of one variant to the suspension point required 2.5 h, while calculation of the complete variant required 4-5 h of machine time (ES 1055 computer).

3. Thorough calculation of all stages of evolution of the thermal was performed for the dimensionless parameters  $\gamma = 1.4$ ,  $M = 0.23$  ( $1/\gamma M^2 = 13.5$ ),  $\text{Re} = 20.4$ ,  $\text{Pr} = \text{Sc} = 1.0$ ,  $H = 2.63$ ,  $\Theta_0 = 21.0$ ,  $k_1 = 7.27 \cdot 10^{-3}$ ,  $k_2 = 2.66 \cdot 10^{-2}$ ,  $H_t = 26.9$ . These parameters correspond, for example, to the cloud formed by an explosion of the power  $W = 4.18 \cdot 10^9$  MJ at an elevation of 1560 m ( $R = 594$  m,  $T_0 = 273$  K,  $p_0 = 0.1$  MPa).

The dynamics of the ascent of the upper edge of the thermal is shown in Fig. 1 in the form of the relation  $z_e(t^{1/2})$ : the solid curve shows theoretical results, the points and

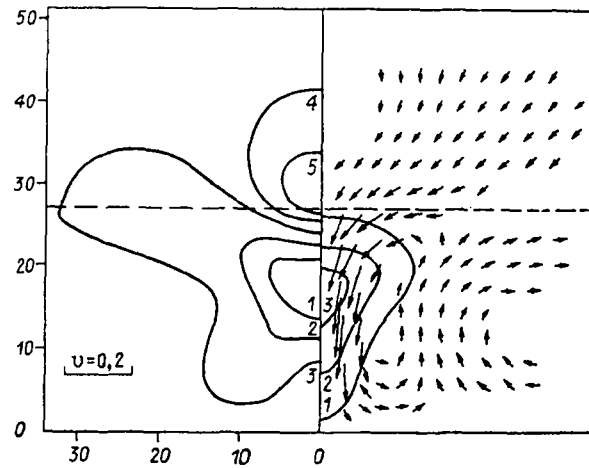


Fig. 5

dashed line show experimental data [1, 15], and the horizontal dashed line shows the position of the tropopause.

All of the above-described main stages are seen in succession in the ascent of the thermal. In the initial stage ( $t \leq 5.9$ ), the thermal is "accelerated" and makes a smooth transition to the similarity stage ( $5.9 \leq t \leq 19.5$ ). The similarity stage is characterized by the presence of a linear section of the relation  $z_e(t^{1/2})$ . Then the suspension stage begins. This stage was calculated until half the period of the first oscillation.

Good agreement was obtained between the experimental and theoretical results over a large time interval. The curves begin to diverge markedly at the suspension stage. An analysis of the empirical relation [1, 15] shows that, beginning with an altitude of about 16 km, there is an increase in the rate of ascent of the thermal. However, in the calculations, its rate of ascent decreases monotonically. Thus, the altitudes at which the thermal is suspended turn out to be different. The difference in the results for high altitudes is evidently due to the fact that the theoretical value of the stratification parameter does not conform to the experimental value (there was no such data in [1, 15]). It should be noted that at the suspension stage, when the temperature of the cloud is close to the temperature of the atmosphere and the rate of convective motion generated by the thermal is low (for the specific example examined above, the velocity of the gas at this stage does not exceed 10-15 m/sec, while it is 100-160 m/sec at the initial and similarity stages), such neglected factors as wind, updrafts, etc. may have a significant effect.

Let us proceed to detailed examination of the individual stages of evolution of a thermal. In the initial stage, the heated gas induces the surrounding medium to move, which in turn leads to the formation of a toroidal vortex flow. Here, the initially spherical cloud is transformed into the characteristic mushroom-shaped structure. The regions of maximum temperature and maximum density of the impurity are located near the symmetry axis. The maximum rate of ascent ( $v \sim 2.1-2.2$ ) of the gas is attained on the axis. The structure of the thermal at the moment  $t = 4.49$  is shown in Fig. 2. Isolines of excess temperature  $\Theta = T - T_a$  ( $\Theta = 0.13, 0.26, 0.39, 0.52, 0.65$ ; curves 1-5) are shown on the left, while isolines of the density of the impurity  $\rho_2$  are shown on the right. The arrows indicate the velocity field. Here and below, the values of  $\rho_2$  on the isolines are equal to  $1/6, 3/6$ , and  $5/6$  of the maximum value of the quantity  $\rho_{2m}$  at the given moment (at  $t = 4.49$ ,  $\rho_{2m} = 0.10$ ). The same pattern holds for the isolines in Figs. 3-6.

At the similarity stage of ascent, the cloud expands and remains roughly the same in shape as previously. The toroidal vortex increases in size and rises together with the thermal. The regions of maximum temperature and maximum density of the impurity move from the axis to the periphery. Meanwhile, as was noted in [6], the center of vorticity does not coincide with the hottest region. Although the gas in the cloud cools, supercooling does not occur. The temperature of the thermal remains higher than the temperature of the atmosphere. The structure of the flow at the moment  $t = 14.7$  is shown in Fig. 3 ( $\Theta \cdot 10^2 = 0.8, 1.7, 2.7, 3.7, 4.6$ ; lines 1-5,  $\rho_{2m} = 1.4 \cdot 10^{-2}$ ).

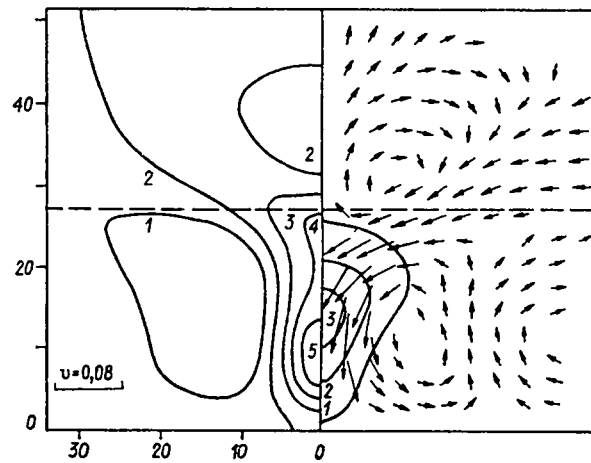


Fig. 6

The final stage is characterized by relatively small temperature gradients. At this stage, a large role begins to be played by stratification of the atmosphere; stable stratification ( $N^2 > 0$ ) results in suspension of the cloud at a certain altitude, with the cloud undergoing thermogravitational oscillations relative to this equilibrium position [4].

The intensive ascent of the gas formed near the axis in the flow in the first two stages leads to a situation whereby the gas passes through the equilibrium position with respect to inertia and is supercooled relative to the atmosphere. The temperature field undergoes inversion: a region with a lower temperature is formed on the symmetry axis, while hotter gas is located at the periphery. As before, the velocity field is toroidal (a single vortex with gas rising at the axis and descending at the periphery).

Subsequent continuing ascent of the gas leads to complete supercooling of the cloud and the nucleation of a secondary vortex above the first vortex. The rotation in the second vortex is opposite the rotation in the first vortex. The point of maximum ascent of the cloud corresponds to a system of two vortices of roughly equal intensity (Fig. 4:  $t = 39.5$ ;  $\Theta \cdot 10^2 = -2.6, -1.9, -1.4, -0.8, -0.3$ ; lines 1-5,  $\rho_{2m} = 2.5 \cdot 10^{-3}$ ). Since the cloud now contains colder, heavier gas, it begins to descend under the force of gravity. Here, the initial vortex is shifted to the periphery, while the secondary vortex expands. The latter embraces the axial region, where a descending gas flow is formed (Fig. 5,  $t = 56.6$ ,  $\Theta \cdot 10^3 = -7.0, -3.7, -0.4, 3, 6.3$ ; lines 1-5,  $\rho_{2m} = 2.3 \cdot 10^{-3}$ ).

The subsequent evolution of the vortex pattern is similar to that described above. The cloud again passes through the inertial equilibrium point as it descends and is then superheated with respect to the atmosphere. A system of oppositely-twisted vortices is again formed at the lowest point (Fig. 6:  $t = 73.5$ ;  $\Theta \cdot 10^3 = -0.8, 1.5, 3.7, 5.9, 8.2$ ; lines 1-5,  $\rho_{2m} = 2.2 \cdot 10^{-3}$ ), the gas begins to ascend on the axis and lift the thermal, etc.

Thus, thermogravitational oscillations of the cloud are accompanied by the formation of a periodically restructured system of large-scale vortices in which the direction of rotation of the main vortex changes (reverses). The uppermost and lowermost positions of the cloud correspond to a system of oppositely-twisted vortices, while the moments at which the equilibrium position is passed correspond to the presence of one vortex in which the axial direction of the gas coincides with the direction of the cloud.

It was noted in [4] that the stratosphere more strongly suppresses ascending convective flows, since the air above the tropopause is nearly isothermal and the gas more quickly loses buoyancy. As a result, when the thermal reaches the stratosphere, the cloud is intensively "diffused" over the tropopause. The sample through calculation described in the present article pertains to the case when the main part of the thermal at the suspension stage is located in the troposphere. Thus, this diffusion is not manifested.

#### LITERATURE CITED

1. A. T. Onufriev, "Theory of motion of a vortex ring under the influence of gravity. Ascent of a cloud from a nuclear explosion," *Zh. Prikl. Mekh. Tekh. Fiz.*, No. 2 (1967).

2. J. S. Turner, Buoyancy Effects in Fluids, Cambridge Univ. Press (1973).
3. E. L. Kogan, I. B. Mazin, B. N. Sergeev, and V. I. Khvorost'yanov, Numerical Modeling of Clouds [in Russian], Gidrometeoizdat, Moscow (1984).
4. Yu. A. Gostintsev, V. V. Lazarev, A. F. Solodovnik, and Yu. V. Shatskikh, "Turbulent thermal in a stratified atmosphere," Preprint, Inst. Khim. Fiz. Akad. Nauk SSSR, Chernogolovka (1985).
5. Yu. P. Glagoleva, V. A. Zhmailo, V. D. Mal'shakova, et al., "Formation of a circular vortex in the surfacing of a light gas in a heavy gas," ChMMSS, 5, No. 1 (1974).
6. V. A. Andrushchenko, Kh. S. Kestenboim, and L. A. Chudov, "Motion of a gas caused by a point explosion in a nonuniform atmosphere," Izv. Akad. Nauk SSSR Mekh. Zhidk. Gaza, No. 6 (1981).
7. V. A. Andrushchenko, Kh. S. Kestenboim, and L. A. Chudov, "Calculation of the ascent and interaction of thermals in the atmosphere (axisymmetric and three-dimensional problems)," in: Turbulent Jets [in Russian], Tallin (1985).
8. G. M. Makhviladze and I. P. Nikolova, "Development of a combustion center in a reacting gas under conditions of natural convection," Preprint, Inst. Probl. Mekhaniki, No. 189, Moscow (1981).
9. G. M. Makhviladze and O. I. Melikhov, "Dynamics and settling of a nonisothermal gas-suspension cloud," Preprint, Inst. Probl. Mekhaniki, No. 207, Moscow (1982).
10. G. M. Makhviladze and S. B. Shcherbak, "Numerical calculation of gasdynamic processes accompanying the combustion of condensed matter," Fiz. Goreniya Vzryva, No. 4 (1980).
11. Yu. A. Gostintsev, G. M. Makhviladze, and O. I. Melikhov, "Entrainment of aerosol particles into the stratosphere by a hot thermal," Izv. Akad. Nauk SSSR Mekh. Zhidk. Gaza, No. 6 (1987).
12. G. M. Makhviladze, O. I. Melikhov, and S. E. Yakush, "Turbulent axisymmetric thermal in a nonuniform compressible atmosphere. Numerical modeling," Preprint, Inst. Probl. Mekhaniki, No. 303, Moscow (1987).
13. Yu. A. Gostintsev, Yu. S. Matveev, et al., "Physical modeling of turbulent thermals," Zh. Prikl. Mekh. Tekh. Fiz., No. 6 (1986).
14. G. M. Makhviladze and S. B. Shcherbak, "Numerical method of studying nonsteady three-dimensional motions of a compressible gas," Inzh. Fiz. Zh., 38, No. 3 (1980).
15. P. S. Dmitriev (ed.), Effect of Nuclear Weapons [in Russian], Voenizdat, Moscow (1965).

## ASYMPTOTIC ANALYSIS OF INVISCID PERTURBATIONS

### IN A SUPERSONIC BOUNDARY LAYER

V. R. Gushchin and A. V. Fedorov

UDC 532.526

Inviscid perturbations play an important role in the linear theory of stability of supersonic boundary layers. These perturbations are described by nonsteady linearized Euler equations [1, 2]. In numerical calculations conducted in [3] for inviscid two-dimensional perturbations in a plane-parallel boundary layer on a thermally insulated plate, it was found that for incoming flows with a Mach number  $M \geq 3$ , other modes besides the first unstable mode are manifest. The number of modes increases rapidly with an increase in  $M$ , the short-wave (high-frequency) part of the spectrum being filled here. It was found in experiments [4] that the second mode begins to dominate the first mode in the boundary layer on a cone for  $M \geq 5.6$ . The author of [5] recorded unstable high-frequency perturbations in supersonic flow about a cone. In [1], it was suggested that these disturbances are associated with the third and higher modes. The question of the role of higher modes in the agitation of a supersonic boundary layer has not yet been resolved. In connection with this, it is interesting to study their properties both theoretically and experimentally.

Here, we perform an asymptotic analysis of inviscid perturbations in a shortwave approximation. We find the dispersion relation and eigenfunctions for neutral modes with large numbers. Numerical calculations are performed to obtain the stability characteristics for the first four modes in a plane-parallel boundary layer with  $M = 8$ . It is shown that the

---

Moscow. Translated from Zhurnal Prikladnoi Mekhaniki i Tekhnicheskoi Fiziki, No. 1, pp. 69-75, January-February, 1989. Original article submitted November 10, 1987.